

# Measurement of the polarization of the radio emission in air showers with LOFAR.

O. Scholten<sup>\*</sup>, P. Schellart<sup>†</sup>, A. Nelles<sup>†,\*\*</sup>, S. Buitink<sup>†</sup>, A. Corstanje<sup>†</sup>, J.E. Enriquez<sup>†</sup>,  
H. Falcke<sup>†,‡</sup>, J.R. Hörandel<sup>†,\*\*</sup>, J.P. Rachen<sup>†</sup>, S. ter Veen<sup>†</sup>, S. Thoudam<sup>†</sup>, T.N.G.  
Trinh<sup>\*</sup> and The LOFAR Collaboration<sup>‡</sup>

<sup>\*</sup>*KVI-CART, University of Groningen, P.O. Box 72, 9700 AB Groningen, The Netherlands*

<sup>†</sup>*Department of Astrophysics/IMAPP, Radboud University Nijmegen, P.O. Box 9010, 6500 GL Nijmegen, The Netherlands*

<sup>\*\*</sup>*Nikhef, Science Park Amsterdam, 1098 XG Amsterdam, The Netherlands*

<sup>‡</sup>*Netherlands Institute for Radio Astronomy (ASTRON), Postbus 2, 7990 AA Dwingeloo, The Netherlands*

**Abstract.** With the LOFAR antenna array we have measured the polarization footprint of the radio emission from extensive air showers for a large number of single events. The polarization direction is determined from the Stokes parameters integrated over the time duration of the radio pulse. It will be shown that for events for which no thunderstorm activity has been registered the polarization pattern obeys very well the expected characteristics based on a superposition of a geomagnetically-induced transverse current and a charge excess contribution. The core-distance dependence of the ratio of the two contributions is measured. For events where thunderstorm activity is registered, strong deviations from the fair-weather polarization pattern are observed.

**Keywords:** Radio observations, cosmic rays, LOFAR, extensive air showers, polarization, Atmospheric electricity

**PACS:** 96.50.S-; 96.50.sd; 95.55.Jz; 92.60.Pw

## INTRODUCTION

As the result of an intense effort in recent years on modeling radio emission from Extensive Air Showers (EAS), consensus has been reached concerning the most important contributing processes [1]. The main contribution is geomagnetic in origin. It results from the transverse current induced in the shower front through the Lorentz force acting on the electrons and positrons. This current is in the  $\vec{v} \times \vec{B}$  direction where  $\vec{v}$  is the main velocity component of the electrons and positrons, which is along the shower direction, and  $\vec{B}$  is the magnetic field of the Earth. The resulting emission amplitude is polarized in the  $\vec{v} \times \vec{B}$  direction, the direction of the induced transverse current. A secondary contribution results from the charge excess in the EAS. This component of the radio-emission amplitude is polarized in the radial direction [2]. Since the emission occurs from a source moving with the light velocity through a medium, relativistic time compression (sometimes called Cherenkov emission) is important for certain viewing angles to the shower axis. This effect greatly affects the intensity of the radiation but not its polarization. We refer to the contribution of Huege to these proceedings [3] for an up-to-date review. Here we present observations of the polarization footprint of extensive air showers as have been determined with LOFAR that show a clear indication of the two main contributing mechanisms as discussed.

The Low Frequency Array (LOFAR) [4], is a digital radio telescope, observing in the frequency range of 10 - 240 MHz. It consists out of many thousands of antennas. The antennas are grouped in stations, where each core station has 96 Low Band Antennas (LBA) and 48 High Band Antennas (HBA). Each LBA consists of two inverted V-shaped dipoles labeled X and Y. These are aligned along the southwest to northeast and southeast to northwest direction respectively. The LBA are sensitive to the frequency range of 10 - 90 MHz. The sensitivity range of the HBA is 110 - 240 MHz. The approximately 2km diameter LOFAR core consists of 24 such stations with the highest density offered by the six stations located in a 350 m diameter region called the ‘superterp’ near Exloo in the north of The Netherlands. Remote stations may lie at a distance of 1000 km from the core. For the purpose of measuring the radio emission from extensive air showers LOFAR is equipped with ring buffers, that store the raw voltage traces of each individual antenna in the array for up to 5 s. When a trigger is received the ring buffers are frozen and their contents copied over the network to a central storage location. In the observation mode pertinent to this work the trigger is generated by a dedicated particle detector array. The LOFAR Radboud Airshower Array (LORA) [5], consists of 20 scintillator

detectors. A trigger is sent to LOFAR when an air shower is detected with an energy exceeding  $2 \times 10^{16}$  eV. The corresponding radio emission for showers of this energy is at the lower limit of detectability by LOFAR for favorable shower geometries. The particle detector array is located at the superterp where the density of radio antennas is highest which makes the setup ideal for cosmic-ray detections. Radio emission from cosmic rays has been measured in both the LBA and HBA frequency bands [6, 7]. The analysis presented here focusses on the LBA measurements.

## DATA ANALYSIS

A detailed description of the off-line analysis of the data can be found in [6, 8]. Here we summarize the most important steps for the polarization analysis. As a first step the narrow bandwidth radio frequency interference (RFI) is identified and removed. Thereafter the noise power, dominated by Galactic emission, is used to perform a relative gain calibration between all dipoles, independently for the X and Y dipoles. An absolute calibration is currently not yet available at LOFAR.

An initial estimate for the arrival direction of the air shower is derived from the timing in the particle detector array. The calculated geometrical delays for this direction are used to coherently add the signals from all dipoles of one station. This increases the signal-to-noise ratio ( $S/N = \sqrt{P_s/P_n}$  defined in terms of a power ratio) by approximately a factor of square-root of the number of antennas. When a pulse is found with a  $S/N > 3$  the station is marked for further processing. The timing of the radio pulse is used to reconstruct the arrival direction. When this, for more than four stations, agrees with that from the particle array, the event is used for further processing. There are 206 air showers that meet this criterium. Of these some are excluded because they are likely influenced by thunderstorm conditions or because no reliable estimate of the shower core position could be obtained leaving a total of 163 air showers used for the analysis. For each of these the radio pattern is sampled at between 192 and 528 distinct locations.

Essential for the polarization analysis is the implementation of the antenna model as this is strongly dependent on the polarization. The measured time traces of the X and Y dipoles are combined and used to extract the polarization directions [6, 8]  $\hat{e}_\theta$  and  $\hat{e}_\phi$  that are perpendicular to the shower axis given by  $\hat{e}_\nu$ , while correcting for the frequency-dependent complex gain [6, 8]. For the present analysis these are subsequently projected onto the  $\hat{e}_{\vec{\nu} \times \vec{B}}$  and  $\hat{e}_{\vec{\nu} \times \vec{\nu} \times \vec{B}}$  directions. Note that for this procedure it is assumed that the emission has no component along the propagation direction  $\hat{e}_\nu$ . As a final step the antenna positions are projected onto the shower plane, defined as the plane perpendicular to the shower and going through the point where the core of the shower hits ground.

In the polarization analysis [8] we will use the Stokes parameters for convenience,

$$\begin{aligned}
 I &= \frac{1}{n} \sum_0^{n-1} \left( E_{i,\vec{\nu} \times \vec{B}}^2 + \hat{E}_{i,\vec{\nu} \times \vec{B}}^2 + E_{i,\vec{\nu} \times \vec{\nu} \times \vec{B}}^2 + \hat{E}_{i,\vec{\nu} \times \vec{\nu} \times \vec{B}}^2 \right) \\
 Q &= \frac{1}{n} \sum_0^{n-1} \left( E_{i,\vec{\nu} \times \vec{B}}^2 + \hat{E}_{i,\vec{\nu} \times \vec{B}}^2 - E_{i,\vec{\nu} \times \vec{\nu} \times \vec{B}}^2 - \hat{E}_{i,\vec{\nu} \times \vec{\nu} \times \vec{B}}^2 \right) \\
 U &= \frac{1}{n} \sum_0^{n-1} \left( E_{i,\vec{\nu} \times \vec{B}} E_{i,\vec{\nu} \times \vec{\nu} \times \vec{B}} + \hat{E}_{i,\vec{\nu} \times \vec{B}} \hat{E}_{i,\vec{\nu} \times \vec{\nu} \times \vec{B}} \right) \\
 V &= \frac{1}{n} \sum_0^{n-1} \left( \hat{E}_{i,\vec{\nu} \times \vec{B}} E_{i,\vec{\nu} \times \vec{\nu} \times \vec{B}} - E_{i,\vec{\nu} \times \vec{B}} \hat{E}_{i,\vec{\nu} \times \vec{\nu} \times \vec{B}} \right). \tag{1}
 \end{aligned}$$

The summation is performed over  $n = 5$  samples, of 5 ns each, centered around the pulse maximum. Here  $E_i$  is sample  $i$  of the electric field component in either the  $\vec{\nu} \times \vec{B}$  or the  $\vec{\nu} \times \vec{\nu} \times \vec{B}$  polarization direction and  $\hat{E}$  its Hilbert transform.

The degree of polarization is given in terms of the Stokes parameters as  $p = \frac{\sqrt{Q^2 + U^2 + V^2}}{I}$ . From the models one does not expect the polarization direction to change over the duration of the pulse and thus  $p = 1$ . Only due to the interference with noise one expects  $p < 1$ , strongly dependent on  $S/N$ . The data fully support this picture where even at  $4.5 < S/N < 5$  one obtains still  $\langle p \rangle = 0.98$ .

The polarization footprint of a shower, see l.h.s of Fig. 1, shows the polarization of the signal defined as the angle  $\psi = \frac{1}{2} \tan^{-1}(U/Q)$  of the semi-major axis of the polarization ellipse with the  $\vec{\nu} \times \vec{B}$ -axis. The figure shows that the dominant polarization is in the  $\vec{\nu} \times \vec{B}$  direction as expected for geomagnetic emission. In addition there is evidence for a slight deviation due to the charge excess component that induces a radial polarization component. To express the latter more clearly the polarization direction  $\psi$  is plotted v.s.  $\phi'$ , the angle of the antenna position w.r.t. the core of the

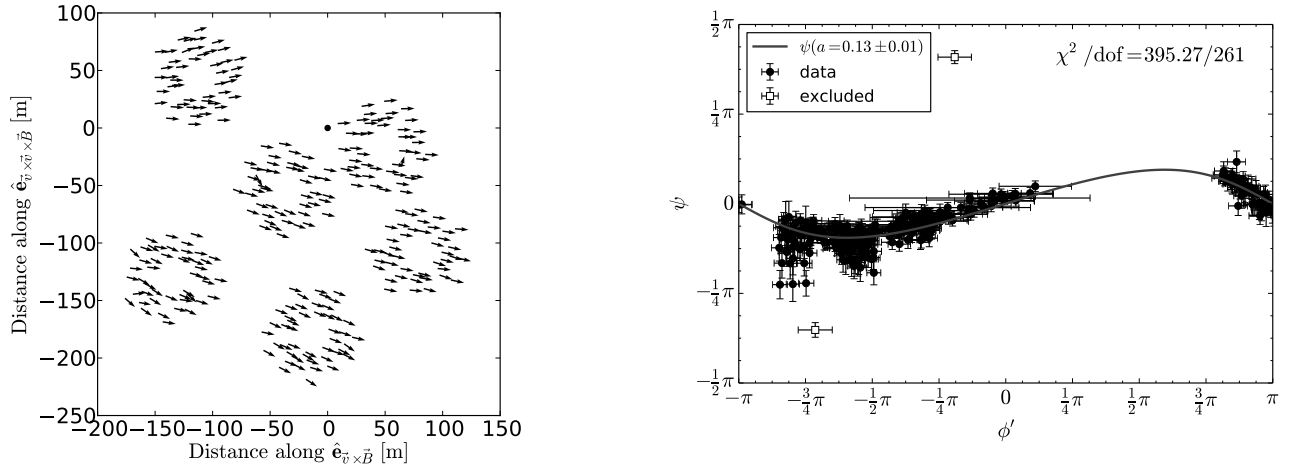


**FIGURE 1.** Left: Polarization footprint of a single air shower, as recorded with the LOFAR low-band antennas, projected into the shower plane. Each arrow represents the electric field measured by one antenna. The shower axis is located at the origin (indicated by the black dot). Right: Polarization angle (defined as the angle with the  $\vec{v} \times \vec{B}$  axis) as a function of azimuth in the shower plane  $\phi'$  for a single air shower. Uncertainties are calculated using a Monte-Carlo procedure. The solid line represents expected dependence for the best fitting value of the radial-polarization fraction  $a$ . Two antennas are excluded from the fit (open squares), since their signals deviate by more than 10 sigma.

shower, as shown on the r.h.s. of Fig. 1. As shown in [2] this is expected to vary in a sinusoidal pattern, consistent with the present measurement.

The ratio between the  $\vec{v} \times \vec{B}$  and the radial polarization components can be expressed as  $a = \sin \alpha |E_C| / |E_G|$  where  $\alpha$  is the angle of the cosmic-ray trajectory with the direction of the magnetic field,  $|E_C|$  ( $|E_G|$ ) is the magnitude of field polarized in the radial (the  $\vec{v} \times \vec{B}$ ) direction, respectively. The drawn curve in Fig. 1 shows the expectation for a constant ratio  $a$ , independent of distance to the shower core for one particular event. One should expect, however, that this ratio is dependent on this distance since the amount of radial polarization should vanish at the core, simply because of symmetry arguments, while the amount of unidirectional polarization may be constant. This simple picture is supported by the data, where in Fig. 2 the mean value of  $a$  is plotted v.s. distance while averaging over all antennas in a certain distance bin from the core for all events. The data show a gradual increase in the ratio with distance and a decrease with zenith angle. To develop a quantitative understanding of these trends simulations are being performed.

## CONCLUSIONS AND OUTLOOK

With LOFAR, complemented with the LORA scintillator array we have the perfect instrument for detailed studies of the radio-footprint of EAS. Here we focussed attention on the polarization of the radio signal and have shown that for fair-weather conditions the data qualitatively supports the model predictions.

Measurements under thunderstorm conditions, defined as an confirmed thunderstorm even by the Dutch weather surface within 2 hours of the measurement, show polarization patterns that are strongly deviating from the fair-weather pattern. The dominant unidirectional polarization points in another direction than  $\vec{v} \times \vec{B}$  and sometimes this differs strongly for the various stations in the footprint. This is the subject of ongoing investigations.

## ACKNOWLEDGMENTS

The LOFAR key science project Cosmic Rays very much acknowledges the scientific and technical support from ASTRON. Furthermore, we acknowledge financial support from the Netherlands Research School for Astronomy (NOVA), the Samenwerkingsverband Noord-Nederland (SNN), the Foundation for Fundamental Research on Matter (FOM) and the Netherlands Organization for Scientific Research (NWO), VENI grant 639-041-130. We acknowledge

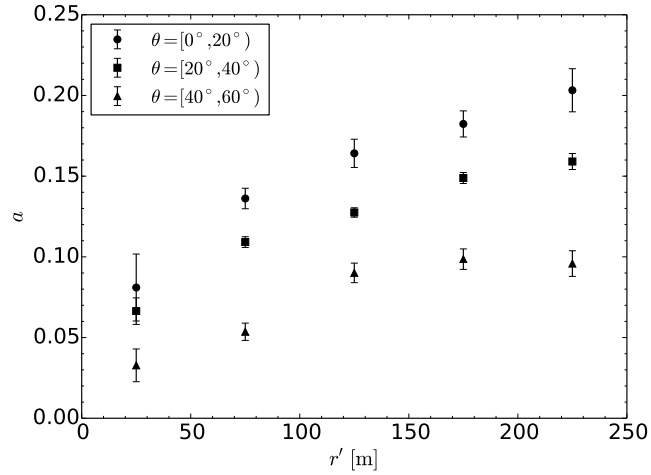


**FIGURE 2.** The radial-polarization fraction  $a$  (conventionally called charge-excess fraction [9]) as a function of distance from the shower axis for three different zenith angle bins.

funding from an Advanced Grant of the European Research Council under the European Unions Seventh Framework Program (FP/2007-2013) / ERC Grant Agreement n.227610.

## REFERENCES

1. T. Huege et al., “The convergence of EAS radio emission models and a detailed comparison of REAS3 and MGMR simulations.”, *Nucl. Instr. and Meth. A* **662**, S179 (2012).
2. K.D. de Vries, et al., *Astropart. Phys.* 34, 267 (2010)
3. T. Huege, these proceedings.
4. M. P. van Haarlem et al., “LOFAR: The LOw-Frequency ARray”, *Astronomy & Astrophysics* **556**, A2 (2013); [arXiv:1305.3550].
5. S. Thoudam et al., “The LOFAR Radboud Air Shower Array”, accepted for publication in *Nuclear Instrument and Methods A* (2014).
6. P. Schellart et al., “Detecting cosmic rays with the LOFAR radio telescope”, *Astronomy & Astrophysics* 560 (Dec., 2013) A98, [arXiv:1311.1399].
7. A. Nelles, P. Schellart et al., “Measuring a Cherenkov ring in the radio emission from air showers at 110-230 MHz with LOFAR”, submitted to *Astroparticle Physics* (2014).
8. P. Schellart et al., “Polarized radio emission from extensive air showers measured with LOFAR”, Submitted for publication, [arXiv:1406.1355].
9. A. Aab, et al., “Probing the radio emission from air showers with polarization measurements”, *Phys. Rev. D* **89**, 052002 (2014); arXiv:1402.3677 [astro-ph.HE].